

Strong Motion and Earthquake Response Records of the 2011 off the Pacific Coast of Tohoku Earthquake

by

Kataoka Shojiro¹, Nagaya Kazuhiro¹, Matsuoka Kazunari² and Kaneko Masahiro³

ABSTRACT

This paper describes strong ground motion and dynamic response of a levee and a viaduct recorded during the 2011 off the Pacific coast of Tohoku earthquake. Iseismal maps have been produced using the strong motion records for developing vulnerability functions of various facilities. Nonlinear response analyses have been carried out for simulating dynamic response of a levee and a viaduct during the earthquake.

KEYWORDS: Levee, Nonlinear Response Analysis, Strong Motion, the 2011 off the Pacific Coast of Tohoku Earthquake, Viaduct

1. INTRODUCTION

The largest earthquake in recorded history in Japan started its rupture on March 11, 2011 at 14:46:18 in JST. Japan Meteorological Agency (JMA) reported JMA magnitude, M_J of the earthquake was 7.9 within 3 minutes. The moment magnitude, M_w was then calculated using data recorded by domestic broadband seismographs but in vain; almost all the data exceeded recording capacity of the seismographs [1].

JMA reported a revised M_J of 8.4 at 16:00 and then M_w of 8.8, which was estimated using data from broadband seismographs all over the world, at 17:30. The M_w was revised to 9.0 on March 13 after a detailed analysis of the rupture process. It was found to include three major ruptures and the maximum slip was estimated to be 40m as shown in Fig. 1 [2].

Challenges left after the earthquake, named the 2011 off the Pacific coast of Tohoku Earthquake by JMA, are so enormous that even its magnitude was hard to be determined as mentioned above. One of the important

challenges is developing methods for effective and economical disaster mitigation against such great earthquakes. In order to gain a foothold for this great task, preliminary analyses were carried out using the strong motions and earthquake response recorded during the devastating earthquake.

2. STRONG MOTION

2.1 MLIT Seismograph Network [3]

Ministry of Land, Infrastructure, Transport and Tourism (MLIT) has been administered the Seismograph Network that consists of more than 700 stations with accelerometers on ground surface since 1997. The stations were installed with intervals of 20 to 40 km along rivers and national highways administered by MLIT. The observed data (PGA, spectrum intensity (SI), and JMA instrumental seismic intensity) are sent to National Institute for Land and Infrastructure Management (NILIM) and opened to the public at NILIM website as shown in Fig. 1 [3].

Fig.2 shows time histories of ground acceleration observed at KSN, OSK, and IWS stations. Two major wave groups at KSN and OSK correspond to the first two ruptures, which occurred near the epicenter, while the peak acceleration at IWS corresponds to the third rupture, which occurred about 200 km south of the epicenter [2]. The data logger of KSN station was installed on the second floor of a two-story building attacked by the tsunami (Photo 1). A little water remained inside of the data logger when it was opened on April 6th.

Fig. 3 compares acceleration response spectra of the ground motion shown in Fig. 2 with those

¹ Senior Researcher, Earthquake Disaster Prevention Division, National Institute for Land and Infrastructure Management, 1 Asahi, Tsukuba 305-0804, Japan

² Researcher, ditto

³ Head, ditto

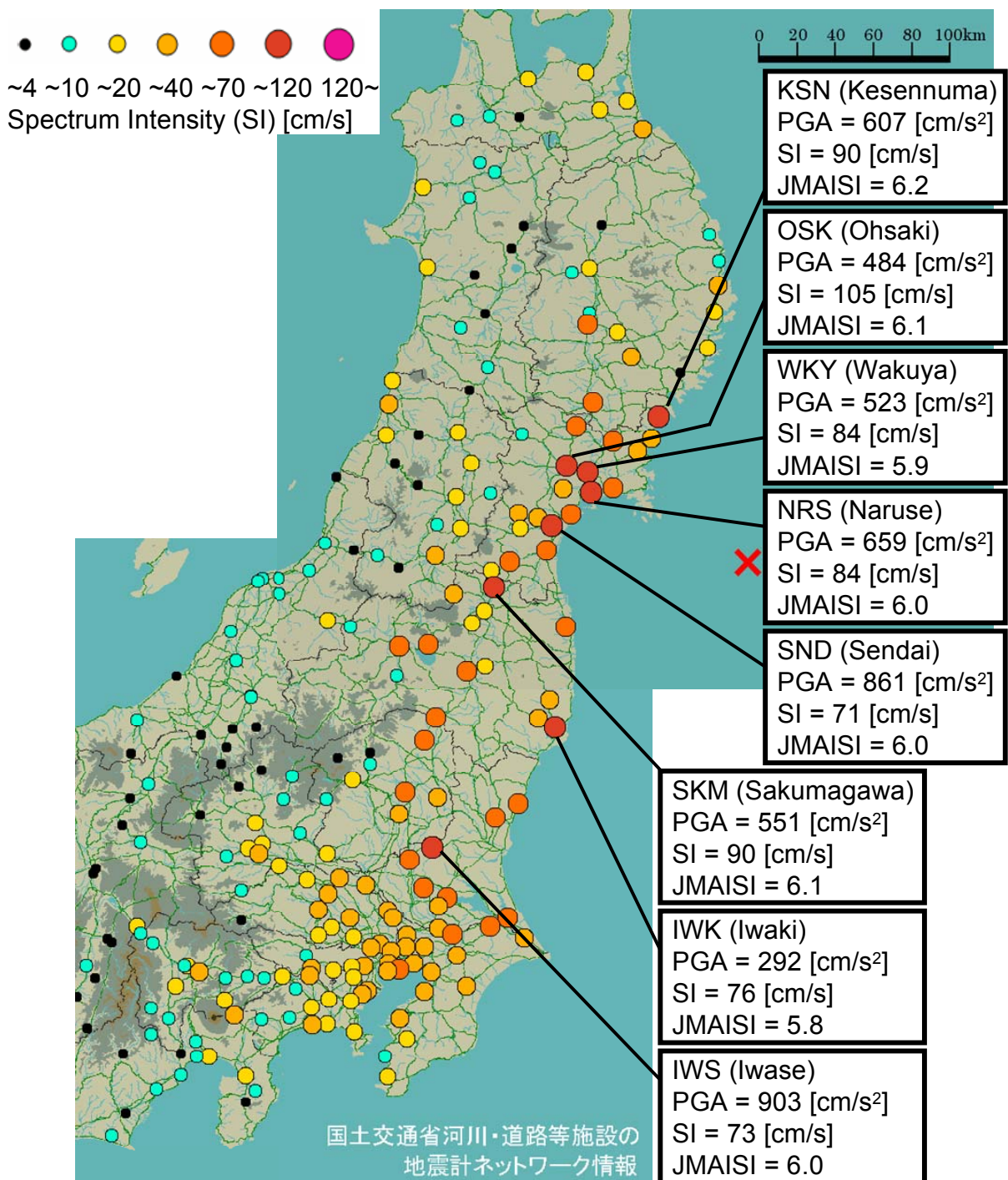


Fig.1 Map of SI observed by MLIT Seismograph Network [3]. PGA, SI, and JMA instrumental seismic intensity are shown for the sites of which SI was 70 [cm/s] or larger. PGA and SI are calculated by synthesizing two horizontal components.

observed at Takatori Station and JMA Kobe Marine Observatory during the 1995 Kobe earthquake. The two response spectra of the 1995 Kobe earthquake are mostly larger than the

other three over the natural period from 0.1 to 10 [s]; this may account for the difference of the damage due to the ground motion (not including tsunami) between these two earthquakes.

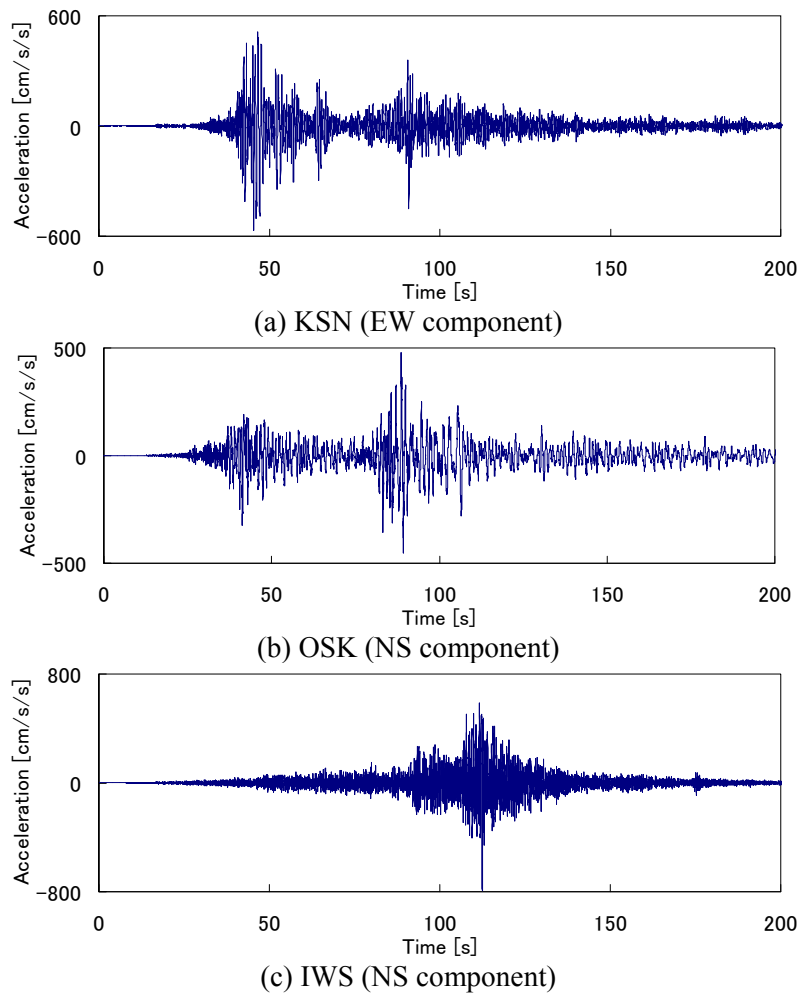


Fig.2 Ground acceleration observed at KSN, OSK, and IWS stations.



Photo 1 Data logger of KSN station that was attacked by tsunami.

2.2 Isoseismal Maps

Isoseismal maps have been produced for PGA, SI, and JMA instrumental seismic intensity by interpolation of strong motion records obtained by MLIT, JMA, and National Research Institute for Earth Science and Disaster Prevention

(NIED). Fig.4 shows the SI isoseismal map as an example. The strong motion observation networks of NIED are known as K-NET and KiK-net [4]. These maps will be employed for developing vulnerability functions of various facilities.

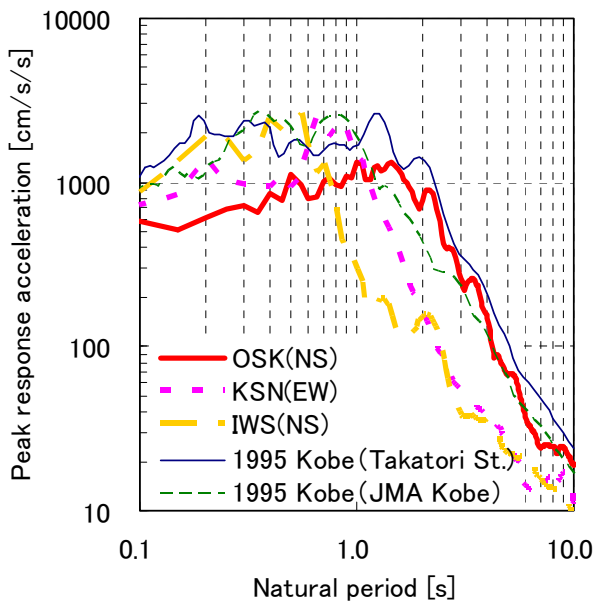


Fig.3 Acceleration response spectra of the strong motion observed at KSN, OSK, and IWS compared with those at Takatori Station and JMA Kobe Observatory of the 1995 Kobe earthquake.

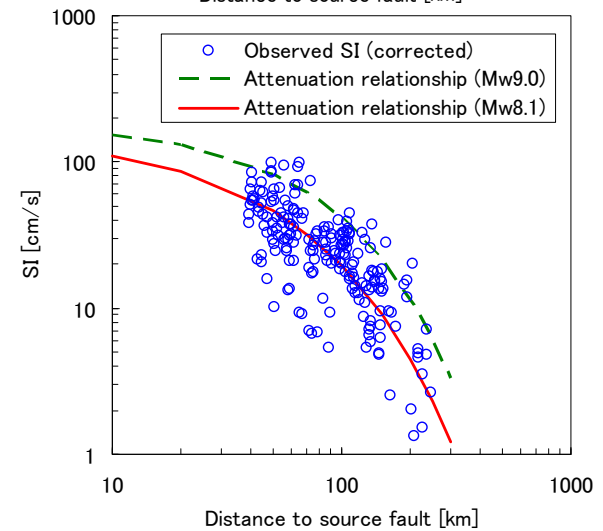
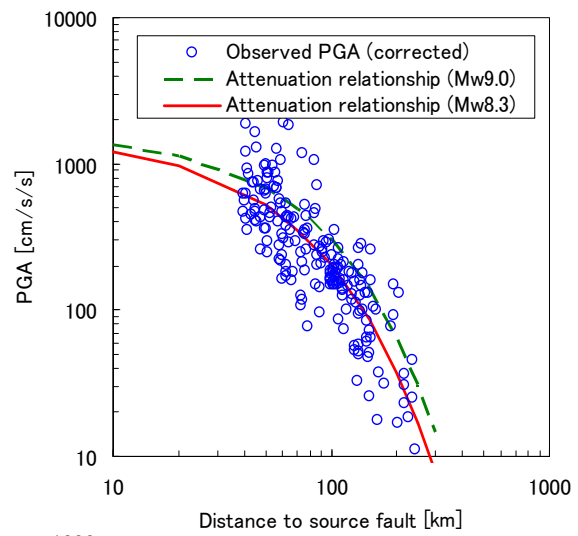


Fig.5 Observed ground motion intensities compared with attenuation relationships [5], which are found to give least errors with the observed PGA and SI when M_w 8.3 and 8.1 are assumed, respectively.

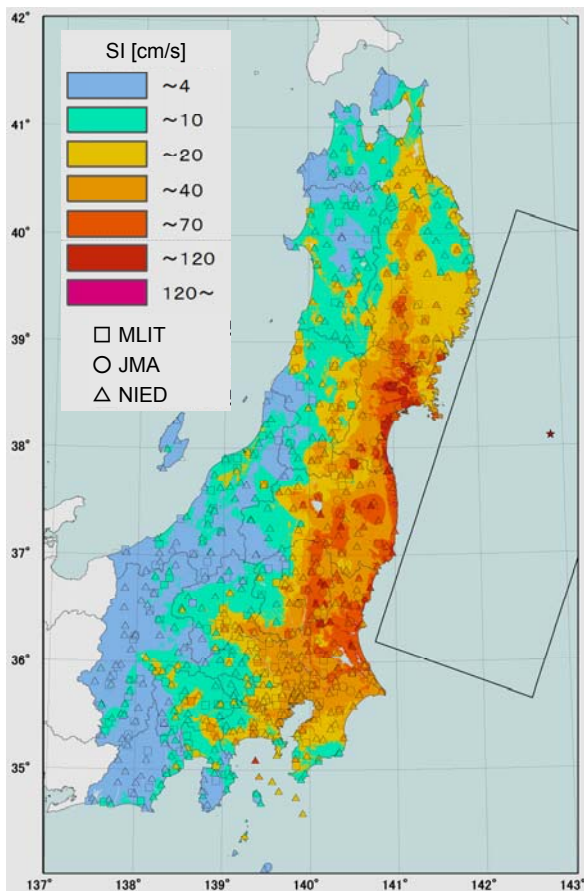


Fig.4 SI isoseismal map based on strong motion records observed by MLIT, JMA, and NIED.

2.3 Ground Motion Attenuation

Fig.5 compares observed ground motion intensities with attenuation relationships [5]. It can be seen that the attenuation relationships overestimate both PGA and SI when M_w 9.0 is assumed. The attenuation relationships are found to have least misfit with the observed PGA and SI when M_w 8.3 and 8.1 are assumed, respectively. Though very large PGAs were observed at several stations within 100km from the source fault, the ground motion during the 2011 off the Pacific Coast of Tohoku Earthquake

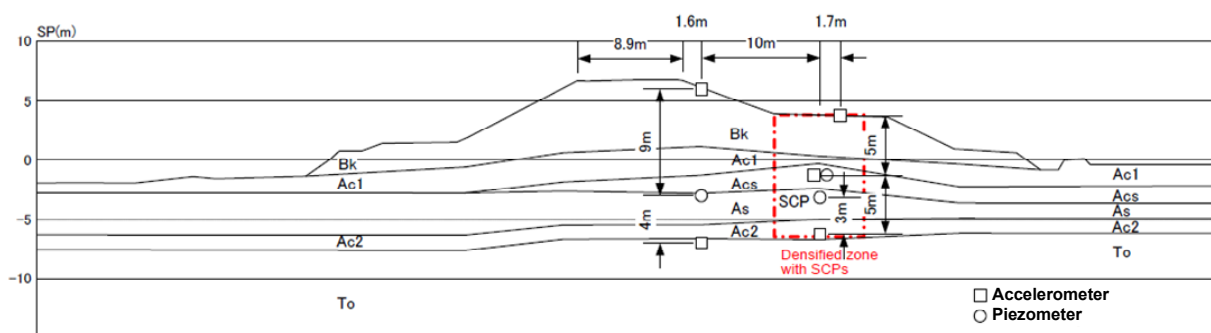


Fig.6 Locations of accelerometers and piezometers at Nakashimo station.



Photo 2 Nakashimo station before (left: 2008) and after (right: April 4, 2011) the earthquake. Tsunami inundation height was about 1m in this area.

in general was not very large considering its magnitude.

3. EARTHQUAKE RESPONSE OF A LEVEE

Fig.6 shows locations of accelerometers and piezometers at Nakashimo station, right-bank of Naruse river, Miyagi prefecture. The sensor arrays were installed at the berm, where liquefaction strength had been improved by the sand compaction pile (SCP) method, and near the crown, where no liquefaction remediation had been conducted.

Time history records of ground acceleration and pore water pressure were obtained at the sensor array near the crown during the 2011 off the Pacific of Tohoku Earthquake, while no records were obtained at the berm. The station was attacked by tsunami, as shown in Photo 2, of

which inundation height was estimated about 1m from the trace of water surface on the inside wall of the instrument shed.

A computer code for 1-D effective stress analysis [6] was employed for the simulation of the earthquake response of the levee. Fig.7 shows the observed motion at the base layer, which was used as an input motion, and the observed and simulated motions at the crown. Though short period component of the simulated motion is somewhat smaller than the observed one, the entire waveform was reproduced well. Observed and simulated time histories of excess pore water pressure are also compared in Fig. 8. Hydrodynamic pressure and dissipation of pore water pressure were not reproduced at all; freezing soil sampling and 2-D simulation may be required for improving the agreement between observed records and the effective stress analysis.

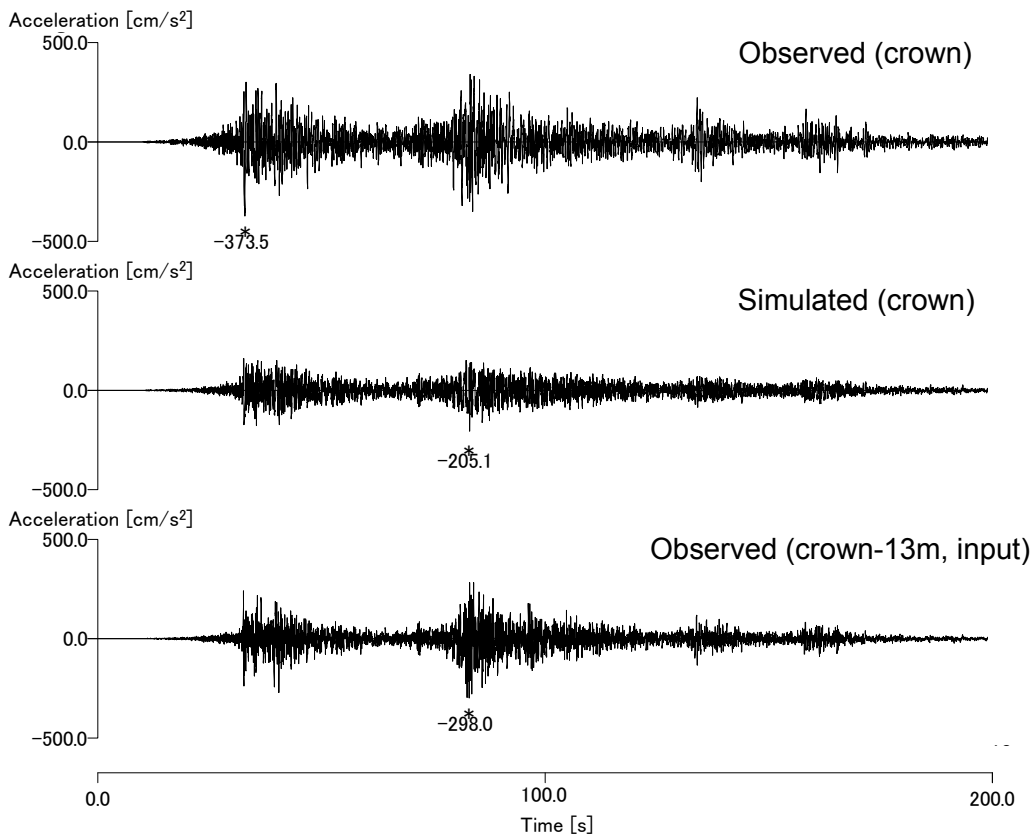


Fig.7 Time history records observed at Nakashimo station during the 2011 off the Pacific of Tohoku Earthquake (NS component, top: crown, bottom: base layer) compared with a simulated motion at the crown by the effective stress analysis (middle).

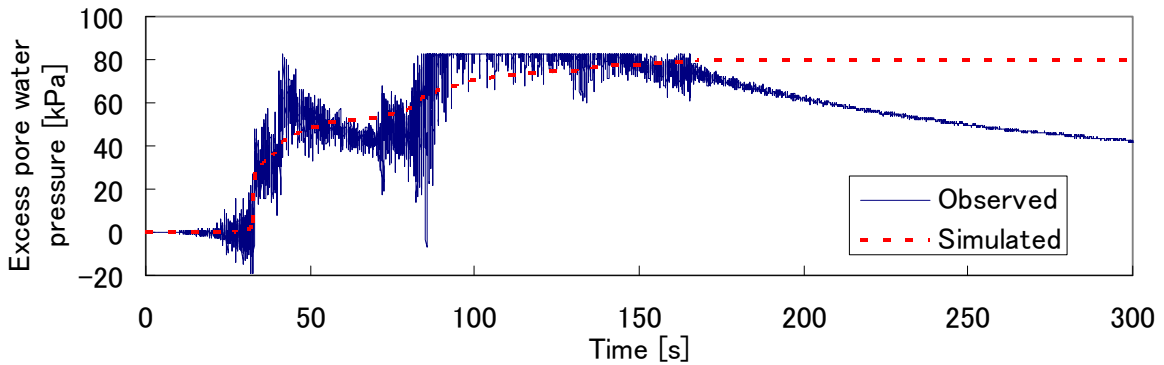


Fig. 8 Observed excess pore water pressure compared with the simulated one.

4. EARTHQUAKE RESPONSE OF A VIADUCT

Fig.9 shows section of Yamada viaduct, 470.7m long with two 4-span continuous steel box girders, using multi-layered rubber bearings. Ground motion and earthquake response of the viaduct were recorded by the accelerometers on

the ground surface, top of P3, and the girder. The accelerograms at the ground surface are shown in Fig.10.

Detailed investigation revealed that side blocks, which had been installed for restricting movement of bearings in the transverse direction,

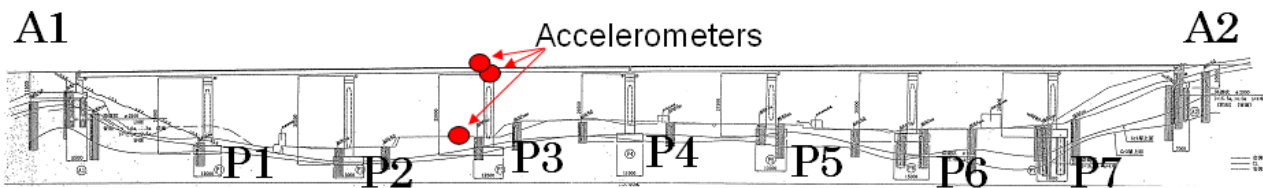


Fig.9 Section of Yamada viaduct with locations of accelerometers.

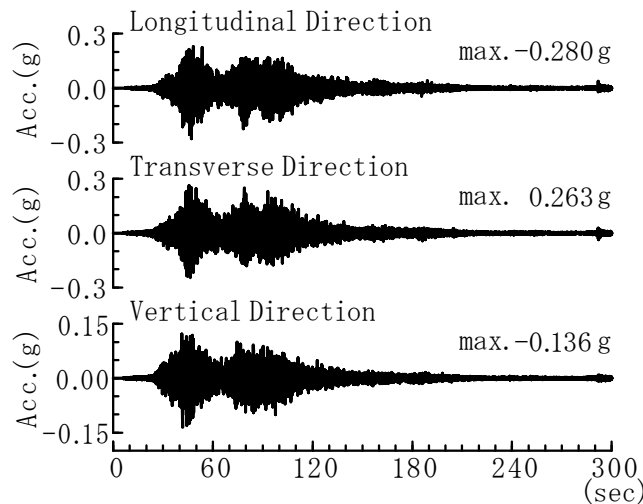


Fig.10 Accelerograms recorded at ground surface under Yamada viaduct.



Photo 3 Yamada viaduct and its bearing. The top plates of bearings were scraped by the side blocks.

scraped top plates of the bearings. Therefore, a dynamic response analysis of the viaduct was carried out taking the contact between the bearings and the side blocks into account (Fig.11).

Figs.12 and 13 compare the observed records with the computed responses. Longitudinal component of the girder and transverse component of the top of P3 are not reproduced

well. We have been investigating the reason that causes the difference between observed and computed responses.

5. CONCLUDING REMARKS

Results of preliminary analyses using the strong motion and earthquake response records obtained during the 2011 off the Pacific of Tohoku Earthquake were presented. Development of

methods for effective and economical disaster mitigation against great earthquakes is a pressing issue. NILIM has been intent on maintenance of the strong earthquake motion observation systems and utilizing the observed records for seismic design and earthquake disaster mitigation. We will be working on further development of the observation systems and improvement of the data utilization.

The strong motion records obtained by JMA, NIED, JR west and MLIT were used in this paper.

6. REFERENCES

1. JMA website: http://www.seisvol.kishou.go.jp/eq/tsunami_kaizen_benkyokai/benkyokai1/si
2. Yoshida, Y., Ueno, H., Muto, D. and Aoki, S.: Source process of the 2011 off the Pacific coast of Tohoku Earthquake, MIS036-P3, 2011.
3. NILIM website: <http://www.nilim.go.jp/japanese/database/nwdb/index.htm>
4. NIED website: <http://www.kyoshin.bosai.go.jp/kyoshin/>
5. Kataoka, S., Satoh, T., Matsumoto, S. and Kusakabe, T.: Attenuation relationships of ground motion intensity using short period level as a variable, *Proc. JSCE, A*, Vol. 62, No. 4, pp. 740-757, 2006.
6. Yoshida, N. and Towhata, I.: YUSAYUSA-2 SIMMDL-2 Theory and usage (version 2.10), 2005.

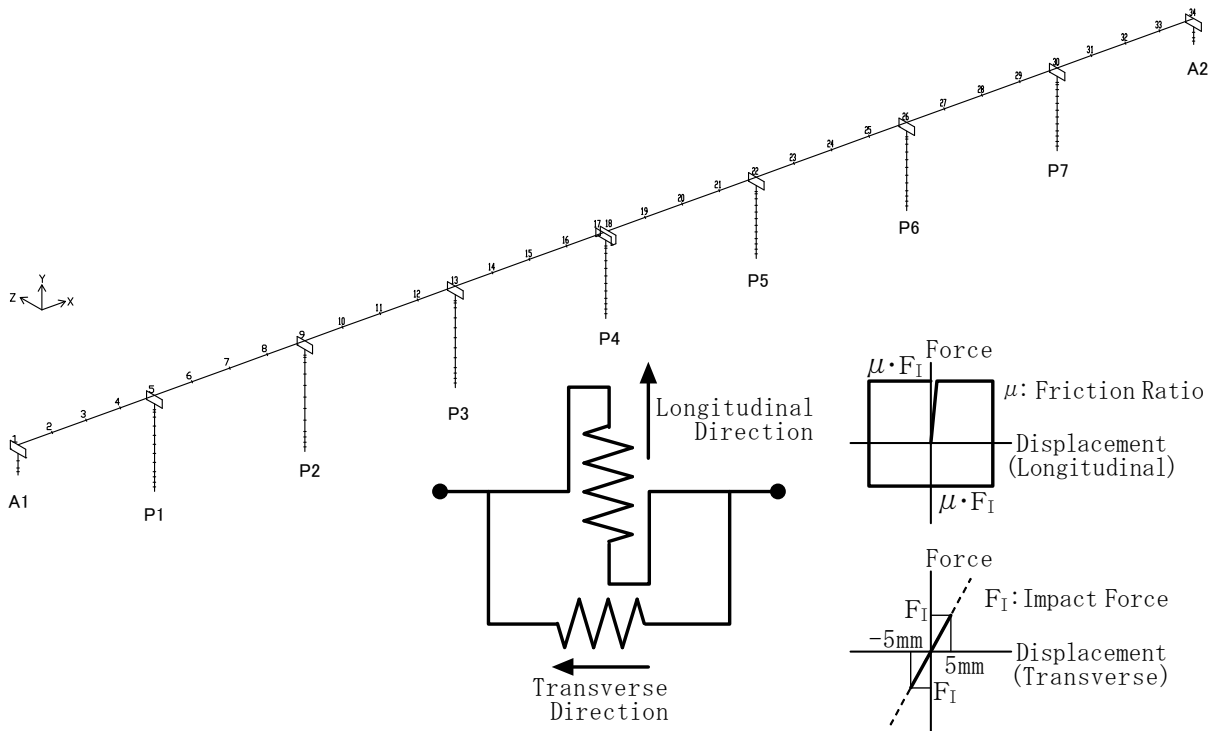


Fig.11 Perspective (top) and force-displacement relationships of bearings with side blocks (bottom) of the analytical model of Yamada viaduct. A sway-rocking model was employed for foundation-ground system.

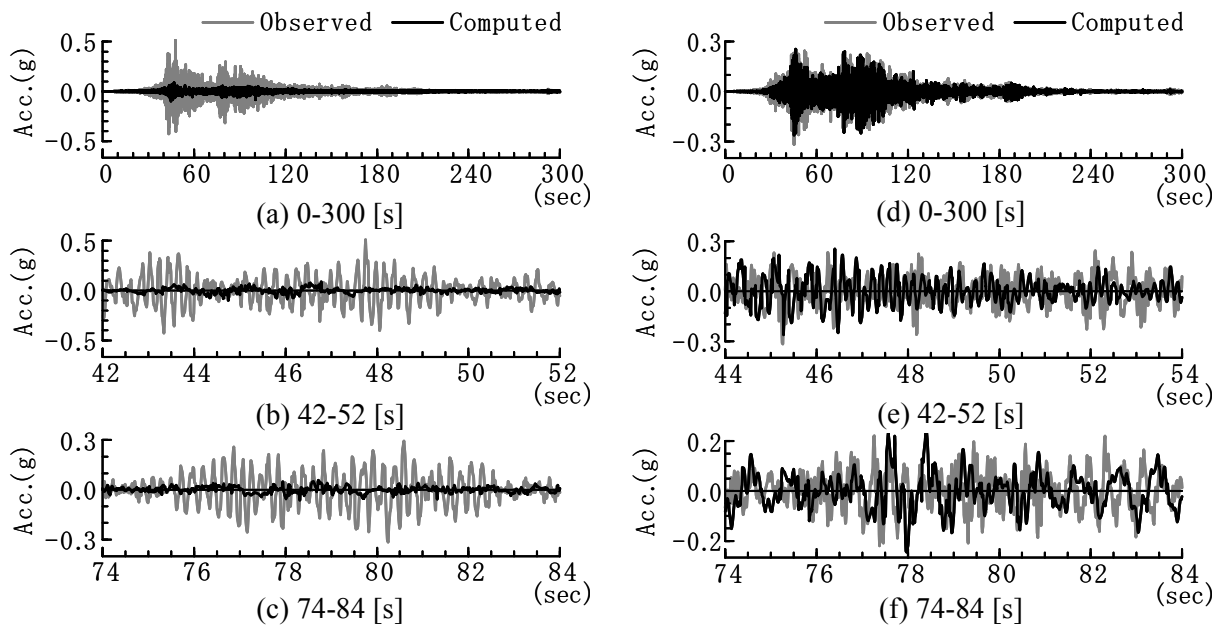


Fig.12 Comparison of the observed and computed earthquake responses of the girder above P3.
 (a)(b)(c): Longitudinal direction; (d)(e)(f): Transverse direction.

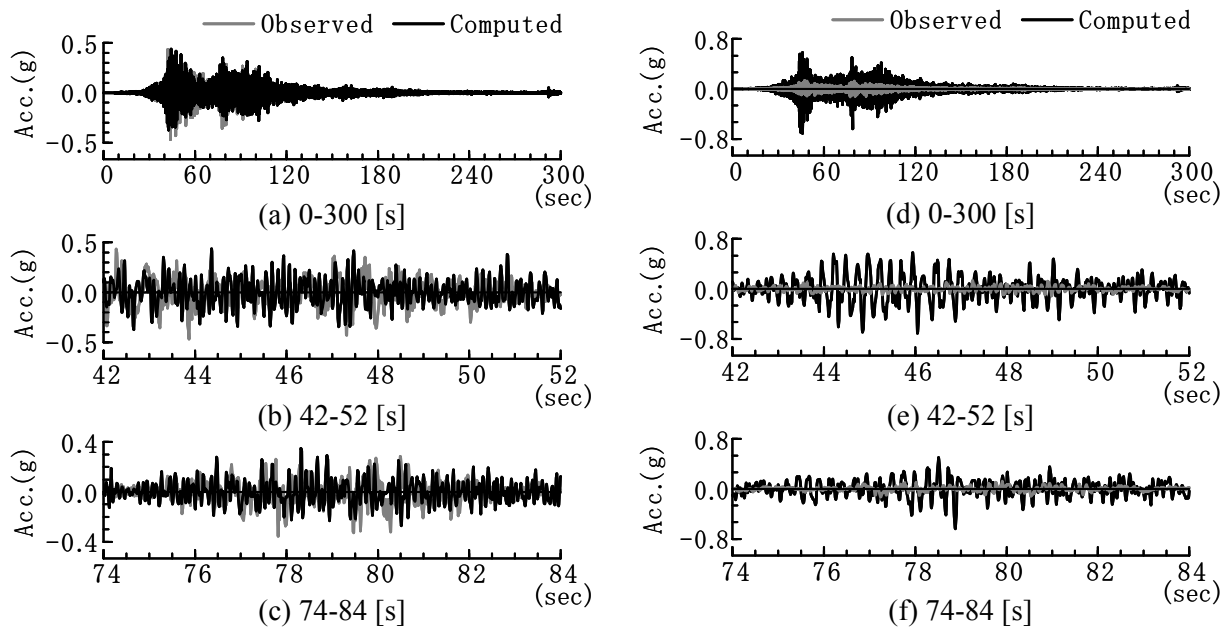


Fig.13 Comparison of the observed and computed earthquake responses of the top of P3.
 (a)(b)(c): Longitudinal direction; (d)(e)(f): Transverse direction.